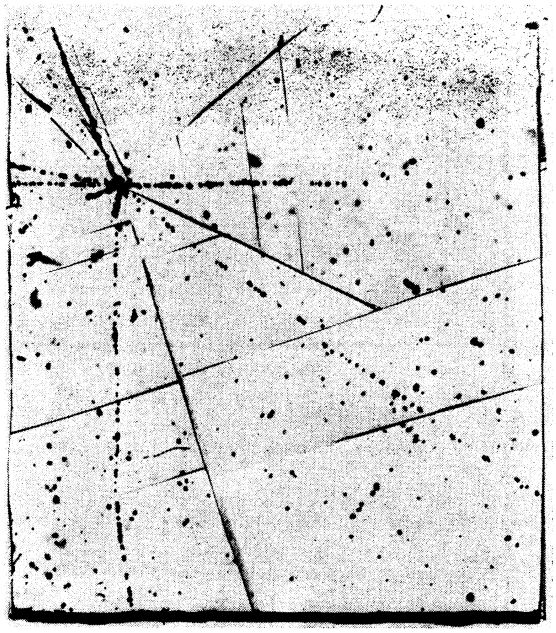

FIG. 2. Enlargement of center section of Fig. 1.

to this track it is pointed out that the coincidence between the star and the track is perfect when examined under the highest magnification. Careful examination leaves no doubt that the grain density increases from right to left indicating that the particle progresses toward the star and does not originate in it. Other possible causes for a change in grain density were considered: Since the track dips 17μ before reaching the end of its range near the center of the 50μ thick emulsion an interpretation other than that of an incident particle would imply

(a) that the deeper layers of the emulsion were more developed than the top layers; but, as is well known, exactly the opposite effect takes place in non-uniform development of nuclear emulsion plates. Furthermore, none of the other tracks indicate any non-uniformity of development; or,

(b) that the top layers of the emulsion have been impaired during the processing. However, no damage to the emulsion could be detected, nor does the appearance of the neighboring star tracks show any irregularities.

By assuming therefore that the star is produced by this particle a lower limit for its mass can be determined from the total energy of the emitted particles. Table I contains a list of the particles emitted in the nuclear disintegration.

Track 8 is of particular interest since grain counts and scattering show that it is produced by a meson coming to rest in the photographic emulsion without producing any visible secondaries. The mass of the meson has been determined as 214 ± 124 electron masses; while no reliance can be placed in the quantitative mass determination of an individual meson this method can be used to distinguish with certainty between a proton and a meson track of the same age. Track 9 is produced by an energetic particle which appears to collide elastically with another particle in the emulsion (9′). From conservation of momentum and energy the ratio of the mass of the incident particle to that of the knock-on is determined as 2.1:1 corresponding to a deuteron proton collision. From the residual range of the scattered deuteron its energy immediately after the collision can be determined as 4.1 Mev. Its energy just before the collision is then calculated from the conservation laws as 18 Mev. From known range energy relations the kinetic energy of the deuteron when leaving the nucleus is found to be 21.1 Mev.** Particles 10 and 11 listed in Table I could not be shown in the photo-micrograph because of the shortness and large angle of dip of their tracks. They are energetic particles which pass out of the emulsion and which have tentatively been identified as protons. (Identification with alpha-particles would yield a higher total energy.)

TABLE I. Particles emitted in the disintegration.

Track number	Track ending	Particle	Kinetic energy (Mev)	Total energy (Mev)
2	glass	alpha	11.3	13.8
3	emulsion	proton	2.2	10.2
4	emulsion	proton	5.6	13.6
5	emulsion	proton	6.3	14.3
6	emulsion	alpha	5.1	7.6
7	emulsion	alpha	2.5	5.0
8	emulsion	meson	2.0	2.0
9	emulsion	deuteron	21.1	23.6
10	air	proton	0.8	8.8
11	air	proton	0.7	8.7

Column 5 in Table I contains the energies of the star particles computed from known range energy relations for the photographic emulsion. In this table the binding energy of protons has been taken as 8 Mev, that of alpha-particles as 2.5 Mev. In the case of particles which do not end in the emulsion the minimum energy is listed, that is, the energy corresponding to the length of track lying entirely in the emulsion. The total energy of the 10 particles is at least 107 Mev.

If the mass of the emitted meson is taken as 285 electron masses the rest mass of the incident particle must be larger than 500 electron masses. The assumption of 210 electron masses corresponding to identification of track 8 with a μ-meson yields, as a lower limit, a mass of 425 electron masses for the incident particle. The actual mass of the particle can only be inferred by speculation; an assumption that the total energy of the star particles not detectable in the photographic plate (particles with minimum ionization and neutral particles) is of the same order of magnitude as that obtained from Table I places the mass of the incident particle in the neighborhood of 700 to 800 electron masses.*** It may be worth mentioning that these mass values yield a lower limit for the lifetime of the particle of the order of 10^{-12} sec.

It is a pleasure to thank Dr. W. Arnquist of the ONR and Mr. C. L. D'Ooge of the Naval Ordnance Test Station at Inyokern, California, for the assistance rendered in exposing the plates.

* The exposure of the plates was made possible through the cooperation of the Pasadena office of the ONR and the Air Force at the Naval Ordnance Test Station at Inyokern, California.

** The alternative that track 9′ is the track of the primary particle and track 9 that of the knock-on can be ruled out. A calculation similar to the one given above yields a mass ratio of 3:1 for the two colliding particles. However, the energy calculated for the triton after the collision would not be sufficient to account for the observed range and ionization of track 9′.

*** A similar event has been reported by Leprince-Ringuet in Rev. Mod. Phys. **21**, 42 (1949).

Thermoelectric Power and Mobility of Carriers in Selenium*

HERBERT W. HENKELS
University of Pennsylvania, Philadelphia, Pennsylvania
December 23, 1949

THE theromoelectric power of single crystal and microcrystalline selenium has been investigated as a function of temperature with parameters of crystallization temperature and oxygen content. Simultaneous measurements of resistivity were made in the cases of the microcrystalline samples. The thermoelectric power of a semiconducting crystal may be related to the density of current carriers, when carriers of one sign and of electronic mass are assumed by:

$$Q=\frac{k}{e}\left(\ln\frac{3\pi T^{\frac{3}{2}}}{8en}-5.32\right). \quad (1)$$

Our previous work on the dark resistivity of "pure" hexagonal microcrystalline selenium has shown that the resistivity and activation energy depend on the temperatures of quench and crystallization. Quenched samples, crystallized rapidly (i.e., at higher temperatures), exhibited very marked non-equilibrium conditions in the temperature dependence of resistance. Both positive and negative temperature coefficients were obtained in different temperature ranges as has been previously reported by other investigators. However, samples prepared without quenches always have negative temperature coefficients. The resistivities of the single crystals have been reported previously.[1]

The thermoelectric power was checked with different temperature gradients but most of the measurements were made with a gradient of approximately 25°C. Figure 1 gives data on the thermoelectric power and resistivity of differently crystallized samples including a single crystal grown from a melt. Figure 2 presents data on the simultaneous measurement of thermoelectric power and resistivity as a function of oxygen content.

Although the relation (1) is not obviously applicable to any microcrystalline aggregate, it should hold for single crystals. However, it is noticed that the behavior of the thermoelectric power is similar for the single crystal and microcrystalline samples. It should be noted that all selenium samples, including single crystals, exhibit to some extent the existence of non-equilibrium conditions. In what follows it must be assumed that in the individual temperature intervals used to measure the thermoelectric power the "acceptor" densities are constant and there are activation energies constant in the small intervals. In a few cases the temperature was raised to within a few degrees of the melting point but the thermoelectric power showed no tendency to reverse or decrease sharply.

An estimate of the density of carriers in different temperature ranges was obtained by use of the formula. The densities calculated are given in Table I, while Table II gives the corresponding mobilities.

To our knowledge there is in the literature no data on the mobility of carriers in single crystal selenium for comparison.

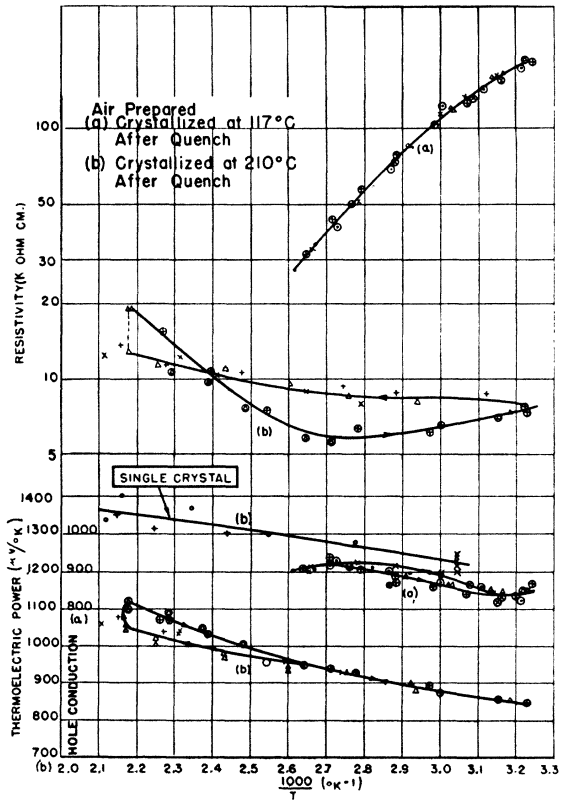

FIG. 1. Resistivity and thermoelectric power of various samples of microcrystalline selenium.

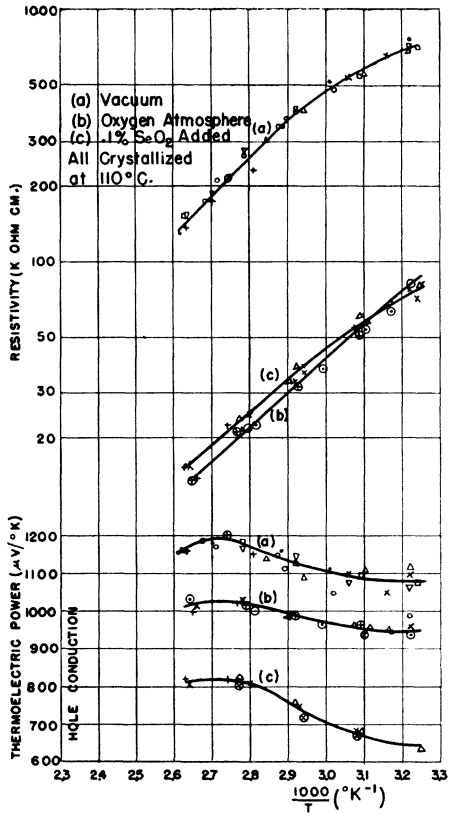

FIG. 2. Thermoelectric power and resistivity of microcrystalline selenium as functions of oxygen content.

TABLE I. Density of carriers in selenium (cm^{-3}).

	50°C	100°C	190°C
Single crystal sample	1.5×10^{14}	1.0×10^{14}	0.6×10^{14}
Microcrystal samples, Lot A			
(a) Air prepared, quenched, crystallized at 110°C	1.1×10^{16}	6.1×10^{15}	——
(b) Air prepared, quenched, crystallized at 210°C	9.9×10^{15}	4.8×10^{15}	1.0×10^{15}
Microcrystal samples, Lot B			
(a) vacuum prepared	7.2×10^{14}	2.7×10^{14}	——
(b) Oxygen atmosphere prepared	3.6×10^{15}	2.0×10^{15}	——
(c) 0.1 percent SeO_2 added, all quenched, crystallized at 110°C	9.2×10^{16}	1.9×10^{16}	——

TABLE II. Mobility of carriers in selenium (cm^2/volt sec.).

		50°C	100°C	190°C
Single crystal sample	$\parallel C$ axis	0.4	1	5
	$\perp C$ axis	0.1	0.3	1
Microcystal samples, Lot A				
(a) Air prepared, quenched, crystallized at 110°C		0.004	0.03	——
(b) Air prepared, quenched, crystallized at 210°C		Av. 0.09	Av. 0.2	Av. 0.4
Microcrystal samples, Lot B				
(a) Vacuum prepared		0.02	0.1	——
(b) Oxygen atmosphere prepared		0.03	0.2	——
(c) 0.1 percent SeO_2 added, all quenched, crystallized at 110°C		0.001	0.02	——

Estimates have been made of the mobility of carriers in microcrystalline selenium with carrier densities based on the capacity of rectifiers. In view of the failure of rectifier theory to explain the observed results in selenium rectifiers and the demonstration of the presence of selenides at the intersurfaces of such rectifiers,[2] the results are considered unreliable. The existence of grain boundary resistance in the case of microcrystalline selenium can readily explain the large difference in mobilities of such samples and single crystals.

* This work was done under Naval Contract NObsr 42487.
[1] H. W. Henkels, Phys. Rev. **76**, 1737 (1949).
[2] H. W. Henkels, Proc. Nat. Electronics Conf. **5** (1949).

Production of C^{15}

EMMETT L. HUDSPETH* AND CHARLES P. SWANN
Bartol Research Foundation of the Franklin Institute,† Swarthmore, Pennsylvania
AND
N. P. HEYDENBURG
Carnegie Institution of Washington, Department of Terrestrial Magnetism, Washington, D. C.
January 19, 1950

THE bombardment of C^{14} with deuterons has been shown to yield d,n and d,α reactions, both of which were recently reported.[1] We have utilized the larger generator of the Carnegie Institution of Washington to make bombardments with deuterons of energy up to 2.8 Mev in order to look for the $C^{14}(d,p)C^{15}$ reaction. The mass estimated for C^{15} is[2] 15.0165, which would indicate that this reaction would have a Q-value of about -2 Mev.

A target of $BaCO_3$ (containing about 40 percent C^{14}), of weight about 400 $\mu g/cm^2$, was used in our bombardments.[3] A preliminary check showed that, when bombarding with deuterons of 2.4-Mev energy, a beta-emitter of half-life much greater than that of B^{12} was also formed. We were able to measure the half-life by simply following the activity of the target with a stop-watch; counts were recorded after the bombarding beam had been shut off for varying lengths of time. The results of these observations are shown in Fig. 1, where the data for three separate runs have been combined and averaged. All of the sets of data indicated a half-life of 2.4 seconds, with an estimated error of about 0.3 second. Some scatter in the points is probably caused by non-uniformity of the target and slight variations in bombarding current.

When it was established that the half-life is so much greater than that of B^{12} (formed in the competing (d,α) reaction) it was possible to make absorption measurements on the beta-rays from C^{15} decay—again by taking observations directly after bombardment was stopped. It was found that the extrapolated end point of the beta-ray spectrum corresponds to 4.6 g/cm² of aluminum absorber; this would indicate a beta-ray energy of 8.8 Mev, with a tentatively estimated error of about 0.5 Mev. This value of the energy, together with the half-life measurement, indicates that the postulated $C^{15}-N^{15}$ decay is a first-forbidden transition.

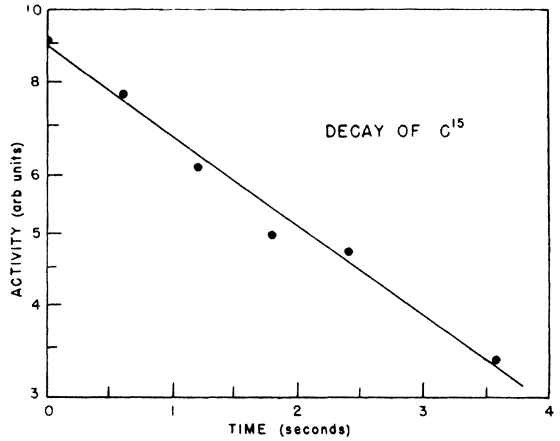

FIG. 1. Activity of C^{15} as measured by counting of beta-rays emitted at various times following deuteron bombardment of C^{14}.

We have also obtained a rough excitation curve; it rises smoothly with increasing energy of deuterons in the region from 1.4 to 2.8 Mev, except for some indication of a resonance at about 1.9 Mev. This, however, must be confirmed.

The calculated mass of C^{15}, based on the beta-ray data, is 15.01434, which makes the Q-value for $C^{14}(d,p)C^{15}$ only slightly negative. However, decay of C^{15} may not be to the ground state of N^{15}, which would alter this mass value as calculated. Indeed, we have some evidence for delayed gamma-emission.

Bombardment of normal $BaCO_3$ was also made, and no beta-emitter of appreciable intensity and of half-life comparable to 2.4 seconds was observed.

More complete details of this investigation will be published in the near future.

* Present address: Department of Physics, University of Texas, Austin, Texas.
† Assisted by the Joint Program of the ONR and AEC.
[1] E. L. Hudspeth and C. P. Swann, Bull. Am. Phys. Soc. **25**, No. 1, 32 (1950), New York Meeting.
[2] H. A. Bethe, *Elementary Nuclear Theory* (John Wiley and Sons, Inc., New York, 1947).
[3] Target material was obtained from Oak Ridge; the estimated value of enrichment was supplied by L. D. Norris (private communication).

Dependence of the F^{19} Nuclear Resonance Position on Chemical Compound*

W. C. DICKINSON
Research Laboratory of Electronics, Massachusetts Institute of Technology, Cambridge, Massachusetts
January 9, 1950

MOST unexpectedly, it has been found that for F^{19} the value of the applied magnetic field H_0 for nuclear magnetic resonance at a fixed radiofrequency depends on the chemical compound containing the fluorine nucleus. The assumption has generally been made that the time average of all internal magnetic fields is zero, excluding of course the small diamagnetic field at the nucleus due to the Larmor precession of its atomic electrons in H_0. Nuclear resonance shifts in metals,[1] interpreted as being due to the conduction electrons, are larger by about an order of magnitude than those reported here.[2]

To investigate the effect in fluorine, two identical magnetic resonance absorption bridges,[3] both fed by the same oscillator, were employed. The two sample holders were placed side by side in the magnet so that the F^{19} resonance traces occurred simultaneously on separate recording milliammeters. This "null" method allows a precision of about 0.0005 percent of the applied field in measuring relative shifts of resonance position and has been used by the author in measuring such shifts due to the addition of paramagnetic ions.

The maximum separation of F^{19} resonances observed so far is 1.05 gauss (see Fig. 1) for $C_2F_3Cl_3$ (freon 113) and BeF_2 in a magnetic field $H_0 \approx 7000$ gauss, the freon resonance coming at the lower *applied* field. Although the resonances in SbF_3 and BeF_2 are separated by 0.99 gauss when observed in separate samples, the separation reduces to 0.82 gauss for a mixture of the two compounds (see Fig. 2). On the other hand, the resonances in SbF_3 and HF are separated by 0.83 gauss in separate samples, but a half and half mixture of the two results in a single resonance located halfway between the positions where the separate resonances would be expected. Increasing the relative amount of SbF_3 shifts